Higgs boson off-shell measurements probe nonlinearities

Anisha,[1,*] Christoph Englert,[1,†] Roman Kogler,[2,‡] and Michael Spannowsky[3,§]
[1]School of Physics and Astronomy, University of Glasgow, Glasgow G12 8QQ, United Kingdom
[2]Deutsches Elektronen-Synchrotron DESY, Notkestr. 85, 22607 Hamburg, Germany
[3]Institute for Particle Physics Phenomenology, Department of Physics, Durham University, Durham DH1 3LE, United Kingdom

(Received 20 February 2024; accepted 23 April 2024; published 22 May 2024)

The measurements of off-shell Higgs boson contributions in massive gauge boson pair production are known to probe its electroweak interactions across different energy scales. Often employed as an estimator of the Higgs boson width in restricted theories of beyond the Standard Model physics, we revisit this measurement and readvertise its potential to constrain aspects of Higgs boson nonlinearity. We show that this so-called off-shell measurement complements related analyses of multi-Higgs final states.

DOI: 10.1103/PhysRevD.109.095033

I. INTRODUCTION

Even some ten years after its discovery, the Higgs boson remains at the core of the experimental quest for new physics beyond the Standard Model (BSM). Given that searches for new states around the TeV scale have so far been unsuccessful, the methodology of effective field theory (EFT) becomes increasingly relevant for the interpretation of Large Hadron Collider (LHC) data, alongside a theoretically useful framing of measurement uncertainties. Most efforts along these lines have concentrated on the so-called Standard Model EFT (SMEFT), largely at the dimension-6 level that constructs effective interactions from SM fields such as the Higgs doublet. As a consequence, SMEFT predicts strict correlations across Higgs multiplicities [1–3]. This, by construction, reduces the qualitative relevance of multi-Higgs production modes as part of a global fit.

From this perspective, in the electroweak chiral Lagrangian (or nonlinear Higgs EFT [4–10], HEFT), any Higgs coupling can be considered a free parameter. On the one hand side, this leads to a significant growth of free parameters, which reduces the value of LHC data as cancellations between couplings naturally imply a loss of sensitivity. On the other hand, existing approaches to analyses pursued by the experimental community can only be interpreted in this framework when SM gauge-related couplings are treated as independent parameters, e.g., in the so-called κ framework [11]. Furthermore, current data still allows for considerable admixture of electroweak singlet states, and associated nonlinearity should be measured and constrained, and not imposed in investigations parallel to the SMEFT program.

How can we constrain such interactions efficiently in the future? Although the aforementioned multi-Higgs programme certainly is an avenue, given the comparably small production cross sections at the LHC, it might not provide a conclusive picture. To this end, we revisit the off-shell Higgs measurement $pp \to 4\ell$ [12] in the context of HEFT. We show that this process, which is usually framed from the perspective of top-Yukawa measurements correlated with the Higgs width under SM assumptions, provides significant power to constrain Higgs boson nonlinearity. This is routed in telltale cancellations of related effects in the context of SMEFT, paired with the nondecoupling of the propagating Higgs contribution as a consequence of unitarity [13].

This note is organized as follows. We highlight a particularly relevant set of interactions that enable the discrimination of SMEFT vs HEFT from nontrivial momentum dependencies that are accessible as part of the off-shell Higgs contribution in, e.g., $pp \to H \to ZZ$ in Sec. II. In Sec. III, we detail all relevant HEFT interactions and their relation to SMEFT, we also comment on details of our implementation. In Sec. IV, we discuss the constraints on Higgs nonlinearity that the off-shell measurement can offer. We conclude in Sec. V.

II. LINEAR VS NONLINEAR MOMENTUM DEPENDENCIES

It is instructive to highlight a particular class of operators that transparently display the differences between HEFT

*anisha@glasgow.ac.uk
†christoph.englert@glasgow.ac.uk
‡roman.kogler@desy.de
§michael.spannowsky@durham.ac.uk

and SMEFT we seek to capitalise on. In the SILH-like basis [14–19] involving only bosonic operators, there is a dimension-6 CP-even operator of class $D^4\Phi^2$ that gives rise to a quartic momentum dependence of the Higgs propagator,

$$Q_{\Box\Phi} = \frac{C_{\Box\Phi}}{\Lambda^2}|D^\mu D_\mu \Phi|^2. \tag{1}$$

Here, Φ is the SM $SU(2)_L$ scalar doublet and D_μ is the covariant derivative. In the broken phase,

$$\Phi = \frac{1}{\sqrt{2}}\begin{pmatrix} 0 \\ v+H \end{pmatrix}, \tag{2}$$

with $v \simeq 246$ GeV. Extending the SM Lagrangian with this dimension-6 operator, in the broken phase, modifies the Higgs two-point function. The corresponding vertex function is written as

$$= -i\Sigma(p^2) = i(p^2 - m_H^2) + i\frac{C_{\Box\Phi}}{\Lambda^2}p^4\,. \tag{3}$$

To obtain the on-shell renormalized Higgs two-point function, the Higgs field is modified as $\sqrt{Z}H = (1+\delta Z_H/2)H$, where Z_H is the Higgs wave function renormalization in the on-shell scheme is given as

$$\delta Z_H = \left.\frac{d\Sigma(p^2)}{dp^2}\right|_{p^2=m_H^2} = -\frac{2C_{\Box\Phi}}{\Lambda^2}m_H^2. \tag{4}$$

Including these corrections, the Higgs propagator becomes [16]

$$\begin{aligned}\Delta_H(p^2) &= \frac{1}{p^2-m_H^2} - \frac{C_{\Box\Phi}}{\Lambda^2} \\ &= \frac{1}{p^2-m_H^2}\left(1 - \frac{C_{\Box\Phi}}{\Lambda^2}\left(p^2-m_H^2\right)\right).\end{aligned} \tag{5}$$

Higher-point functions also receive dimension-6 corrections and the corresponding Feynman rule for, e.g., the HZZ three-point vertex function is

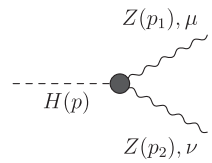

$$= i\Gamma^{\mu\nu}_{HZZ}(p,p_1,p_2)$$

$$= \frac{ie^2 v}{2c_W^2 s_W^2}\left[g^{\mu\nu} + \left(p^2 g^{\mu\nu} - p^\nu p_2^\mu - p_1^\mu p_2^\nu - p^\mu p_2^\nu\right)\frac{C_{\Box\Phi}}{\Lambda^2}\right]. \tag{6}$$

To gain a qualitative understanding of the overall amplitude modification induced by $Q_{\Box\Phi}$ (neglecting all $1/\Lambda^4$ terms), we combine the Eqs. (3) and (6)

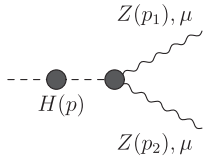

$$= \frac{1}{p^2-m_H^2} g^{SM}_{HZZ}\,, \tag{7}$$

i.e., the momentum-dependent dimension-6 modifications cancel at the leading order in the $1/\Lambda^2$ expansion. This is because the modification correlates the $Q_{\Box\Phi}$ modifications between the broken and unbroken phases [16]. In the linearized approximation, this also removes sensitivity in weak boson fusion signatures that are traditionally telltale signatures of electroweak modifications that temper with unitarity. This cancellation is therefore unique to the way how electroweak symmetry is broken. If the Higgs boson has a singlet component that feels the presence of the HEFT-like operator (see also [20]),

$$\mathcal{O}_{\Box\Box} = \frac{a_{\Box\Box}}{v^2}\Box H \Box H, \tag{8}$$

the cancellation detailed above will not occur. We can therefore expect nontrivial momentum dependencies in HEFT that are not predicted from SMEFT correlations, which can be exploited to set constraints (see also Ref. [21]).

III. HEFT INTERACTIONS, SMEFT RELATIONS, AMPLITUDES

A. HEFT interactions

The leading order HEFT Lagrangian relevant for our study is given by

$$\begin{aligned}\mathcal{L} = &-\frac{1}{4}W^a_{\mu\nu}W^{a\mu\nu} - \frac{1}{4}B_{\mu\nu}B^{\mu\nu} + \mathcal{L}_{\text{ferm}} + \mathcal{L}_{\text{Yuk}} \\ &+ \frac{v^2}{4}\mathcal{F}_H \text{Tr}\left[D_\mu \boldsymbol{U}^\dagger D^\mu \boldsymbol{U}\right] + \frac{1}{2}\partial_\mu H \partial^\mu H - V(H),\end{aligned} \tag{9a}$$

where, the matrix $\boldsymbol{U} = \exp(i\pi^a\tau^a/v)$ defines the Goldstone bosons π^a in a nonlinear parametrization with τ^a being the Pauli matrices for $a = 1, 2, 3$ and its covariant derivative is written as

$$D_\mu \boldsymbol{U} = \partial_\mu \boldsymbol{U} + ig_W(W^a_\mu\tau^a/2)\boldsymbol{U} - ig'\boldsymbol{U}B_\mu\tau^3/2. \tag{9b}$$

$\mathcal{F}_H$ is the flare function giving the Higgs interactions with gauge and Goldstone bosons and is given as

$$\mathcal{F}_H = \left(1 + 2(1+\zeta_1)\frac{H}{v} + (1+\zeta_2)\left(\frac{H}{v}\right)^2 + \cdots\right). \tag{9c}$$

The couplings of Higgs boson with fermions are

$$\mathcal{L}_{\rm Yuk} = -\frac{v}{\sqrt{2}}\begin{pmatrix}\bar{u}_L^i & \bar{d}_L^i\end{pmatrix}\boldsymbol{U}\begin{pmatrix}\mathcal{Y}_{ij}^u u_R^j \\ \mathcal{Y}_{ij}^d d_R^j\end{pmatrix} + \text{H.c.}, \tag{9d}$$

and $\mathcal{Y}_{ij}^f$ is the function similar to $\mathcal{F}_H$ denoting the Higgs fermion interactions as

$$\mathcal{Y}_{ij}^f = y_{ij}^f\left(1 + \left(1 + a_{1f}\right)\frac{H}{v} + \cdots\right). \tag{9e}$$

The light quarks and leptons are neglected throughout our work. Here, y_{ij}^f are the Yukawa couplings directly related to the mass terms. This leading-order HEFT Lagrangian can be extended by the chiral dimension-4 operators tabled in Table I reflect generic BSM connected to a custodial singlet nature of the Higgs boson. These interactions will be sourced at one-loop order from the leading order (chiral dimension-2) Lagrangian, Eq. (9), see [22–25] and can have significant implications for phenomenological observations [26,27]. For concrete matching computations related to HEFT, see the recent Refs. [28–30].

In our work, we further assume that the electroweak precision constraints are not violated and the oblique S, T, and U parameters [31] are related to the following chiral dimension-4 operators [32],

$$S \propto a_{H1}, \qquad T \propto a_{H0}, \qquad U \propto a_{H8}. \tag{10}$$

Thus, these above-mentioned operators are predominantly constrained from electroweak precision data, and to explore the sensitivity of the off-shell measurement to Higgs nonlinearity, we set these coefficients to zero. (The potential shortfalls of such assumptions in the context of global fits and SMEFT have been highlighted in Ref. [33,34].)

TABLE I. Relevant HEFT operators $\mathcal{O}_i$ with a_i being the corresponding HEFT coefficients. $\boldsymbol{\mathcal{V}}_\mu = (D_\mu \boldsymbol{U})\boldsymbol{U}^\dagger$ and $\mathcal{D}_\mu \boldsymbol{\mathcal{V}}^\mu = \partial_\mu \boldsymbol{\mathcal{V}}^\mu + i[g_W W_\mu^a \tau^a/2, \boldsymbol{\mathcal{V}}^\mu]$.

$\mathcal{O}_{HBB}$	$-a_{HBB} g'^2 \frac{H}{v}\mathrm{Tr}[B_{\mu\nu}B^{\mu\nu}]$
$\mathcal{O}_{HWW}$	$-a_{HWW} g_W^2 \frac{H}{v}\mathrm{Tr}[W_{\mu\nu}^a W^{a\mu\nu}]$
$\mathcal{O}_{\Box\boldsymbol{\mathcal{V}}\boldsymbol{\mathcal{V}}}$	$a_{\Box\boldsymbol{\mathcal{V}}\boldsymbol{\mathcal{V}}} \frac{\Box H}{v}\mathrm{Tr}[\boldsymbol{\mathcal{V}}_\mu \boldsymbol{\mathcal{V}}^\mu]$
$\mathcal{O}_{H0}$	$a_{H0}(M_Z^2 - M_W^2)\frac{H}{v}\mathrm{Tr}[\boldsymbol{U}\tau^3\boldsymbol{U}^\dagger\boldsymbol{\mathcal{V}}_\mu]\mathrm{Tr}[\boldsymbol{U}\tau^3\boldsymbol{U}^\dagger\boldsymbol{\mathcal{V}}_\mu]$
$\mathcal{O}_{H1}$	$a_{H1} g' g_W \frac{H}{v}\mathrm{Tr}\left[\boldsymbol{U}B_{\mu\nu}\frac{\tau^3}{2}\boldsymbol{U}^\dagger W_{\mu\nu}^a\frac{\tau^a}{2}\right]$
$\mathcal{O}_{H8}$	$-\frac{a_{H8}}{4} g_W^2 \frac{H}{v}\mathrm{Tr}\left[\boldsymbol{U}\tau^3\boldsymbol{U}^\dagger W_{\mu\nu}^a\frac{\tau^a}{2}\right]\mathrm{Tr}\left[\boldsymbol{U}\tau^3\boldsymbol{U}^\dagger W_{\mu\nu}^a\frac{\tau^a}{2}\right]$
$\mathcal{O}_{H11}$	$a_{H11}\frac{H}{v}\mathrm{Tr}[\mathcal{D}_\mu\boldsymbol{\mathcal{V}}^\mu\mathcal{D}_\nu\boldsymbol{\mathcal{V}}^\nu]$
$\mathcal{O}_{H13}$	$-\frac{a_{H13}}{2}\frac{H}{v}\mathrm{Tr}[\boldsymbol{U}\tau^3\boldsymbol{U}^\dagger\mathcal{D}_\mu\boldsymbol{\mathcal{V}}_\nu]\mathrm{Tr}[\boldsymbol{U}\tau^3\boldsymbol{U}^\dagger\mathcal{D}^\mu\boldsymbol{\mathcal{V}}^\nu]$
$\mathcal{O}_{d1}$	$i a_{d1} g' \frac{\partial^\nu H}{v}\mathrm{Tr}\left[\boldsymbol{U}B_{\mu\nu}\frac{\tau^3}{2}\boldsymbol{U}^\dagger\boldsymbol{\mathcal{V}}^\mu\right]$
$\mathcal{O}_{d2}$	$i a_{d2} g_W \frac{\partial^\nu H}{v}\mathrm{Tr}\left[W_{\mu\nu}^a\frac{\tau^a}{2}\boldsymbol{\mathcal{V}}^\mu\right]$
$\mathcal{O}_{d3}$	$a_{d3}\frac{\partial^\nu H}{v}\mathrm{Tr}\left[\boldsymbol{\mathcal{V}}^\mu\mathcal{D}_\mu\boldsymbol{\mathcal{V}}^\mu\right]$
$\mathcal{O}_{d4}$	$a_{d4} g_W \frac{\partial^\nu H}{v}\mathrm{Tr}\left[\boldsymbol{U}\tau^3\boldsymbol{U}^\dagger W_{\mu\nu}^a\frac{\tau^a}{2}\right]\mathrm{Tr}\left[\boldsymbol{U}\tau^3\boldsymbol{U}^\dagger\boldsymbol{\mathcal{V}}^\mu\right]$
$\mathcal{O}_{\Box 0}$	$a_{\Box 0}\frac{(M_Z^2 - M_W^2)}{v^2}\frac{\Box H}{v}\mathrm{Tr}[\boldsymbol{U}\tau^3\boldsymbol{U}^\dagger\boldsymbol{\mathcal{V}}_\mu]\mathrm{Tr}[\boldsymbol{U}\tau^3\boldsymbol{U}^\dagger\boldsymbol{\mathcal{V}}_\mu]$
$\mathcal{O}_{\Box\Box}$	$a_{\Box\Box}\frac{\Box H\Box H}{v^2}$

B. SMEFT from HEFT

Some of the operators listed in Table I are related to the following dimension-6 SMEFT operators in the Warsaw basis [35]:

$$\begin{aligned} Q_{\Phi B} &= \frac{C_{\Phi B}}{\Lambda^2}\Phi^\dagger\Phi B_{\mu\nu}B^{\mu\nu}, \\ Q_{\Phi W} &= \frac{C_{\Phi W}}{\Lambda^2}\Phi^\dagger\Phi W_{\mu\nu}^a W^{a,\mu\nu}, \\ Q_{t\Phi} &= \frac{C_{t\Phi}}{\Lambda^2}\left(\Phi^\dagger\Phi(\bar{Q}t\tilde{\Phi}) + \text{H.c.}\right). \end{aligned} \tag{11}$$

Here Q's are the SMEFT operators and C's are the corresponding Wilson coefficients (WCs) with Λ being the cutoff scale. The translation rules between the nonlinear and linear coefficients are

$$\begin{aligned} a_{HBB} &= -2\frac{v^2}{g'^2}\frac{C_{\Phi B}}{\Lambda^2}, \\ a_{HWW} &= -2\frac{v^2}{g_W^2}\frac{C_{\Phi W}}{\Lambda^2}, \\ a_{1t} &= -\frac{v^3}{\sqrt{2}M_t}\frac{C_{t\Phi}}{\Lambda^2}. \end{aligned} \tag{12}$$

We need to go to the higher-mass dimension (larger than $d = 6$) to obtain the correspondence of the other HEFT operators.

C. Amplitudes and implementation

We implement the EFT corrections using form factors [36]. Concretely, we extract the independent Lorentz structures contributing to the Higgs amplitudes decay amplitudes $H \to VV$ after performing on-shell renormalization as described above. The relevant Higgs off-shell $H \to VV$ corrections, including the expanded Higg boson propagator, are then given by

$$\begin{aligned} i\tilde{\Gamma}_{HVV} = &-\frac{e^2 m_t}{2c_W^2 s_W^2}\frac{1}{q^2 - M_H^2 + i\Gamma_H M_H} \\ &\times\left\{\left[(1 + \mathcal{F}_1) + \frac{\mathcal{F}_2}{v^2}\left(q^2 - p_1^2 - p_2^2\right) + \frac{\mathcal{F}_3}{v^2}q^2\right.\right. \\ &\left.\left. + \frac{\mathcal{F}_5}{v^2}\frac{M_H^2}{q^2 - M_H^2 + i\Gamma_H M_H}\right]\left[\varepsilon^*(p_1)\cdot\varepsilon^*(p_2)\right]\right. \\ &\left. + \frac{\mathcal{F}_4}{v^2}\left[\varepsilon^*(p_1)\cdot p_2\right]\left[\varepsilon^*(p_2)\cdot p_1\right]\right\}, \end{aligned} \tag{13a}$$

where we have included the Yukawa coupling alongside its corrections arising from $t\bar{t} \to H(q)$, with $q = p_1 + p_2$

(M_H, Γ_H denote the Higgs boson mass and width, respectively). Matching the Lorentz structures to the HEFT coefficients (which contain a SMEFT limit), we find

$$\mathcal{F}_1 = a_{1t} + 2a_{\Box\Box}\frac{M_H^2}{v^2} + \zeta_1, \tag{13b}$$

$$\mathcal{F}_2 = a_{H13} + 2a_{HBB}s_W^4 + 2a_{HWW}c_W^4, \tag{13c}$$

$$\mathcal{F}_3 = a_{\Box BB} - 2a_{\Box\Box} + a_{d2} + 2a_{d4} + \frac{e^2}{c_W^2}a_{\Box 0} - (a_{d1} - a_{d2} - 2a_{d4})s_W^2, \tag{13d}$$

$$\mathcal{F}_5 = 2a_{\Box\Box}, \tag{13e}$$

$$\frac{\mathcal{F}_4}{2} = (a_{d1} + 4a_{HWW})s_W^2 - 2a_{HWW} - (a_{d2} + 2a_{d4})c_W^2 - 2(a_{HBB} + a_{HWW})s_W^4, \tag{13f}$$

for $H \to ZZ$. A similar decomposition holds for $H \to WW$. $\mathcal{F}_5$ arises from corrections to the Higgs propagator, Eq. (5). As this is obtained from the 2-point vertex function (i.e., the inverse propagator), the corrections related to $\mathcal{F}_5$ are intrinsically dependent on the truncation at chiral dimension-4 (equivalent to dimension-6 for the SMEFT identification). To some extent $\mathcal{F}_5$ therefore probes a truncation scheme dependence, in particular in the off-shell regime where the LHC experiments perform their measurement $q \gtrsim 350$ GeV. Sensitivity to $\mathcal{F}_5$ is comparably suppressed to the other $\mathcal{F}_i$, and we can therefore trust the truncation as detailed here, Fig. 1. The amplitudes and their corrections relative to the SM have been implemented using VBFNLO [37,38] (including cross-checks against the results of [39,40]). For this study we limit ourselves to linear new physics contribution, i.e., the differential cross sections are truncated at linear order of the HEFT coefficients.

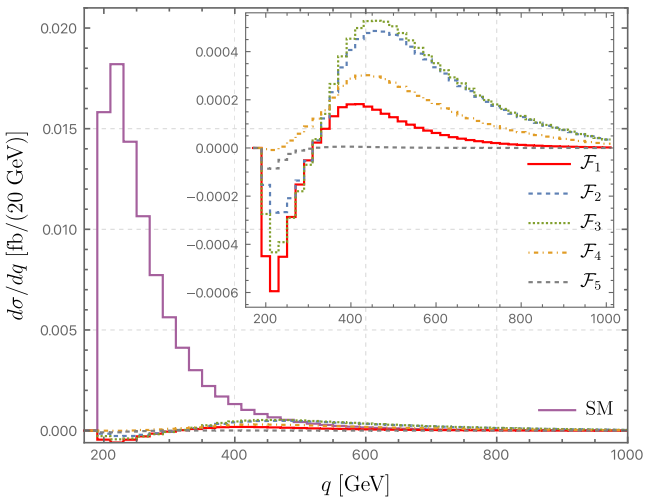

FIG. 1. Off-shell Higgs momentum distributions for $H \to ZZ$ for SM and with the different form factors $\mathcal{F}_i = 1$ shown in the inset.

The phenomenological significance of the off-shell measurement lies in its correlation with on-shell Higgs quantities. For instance, Eq. (13a) introduces modifications to the Higgs branching to vector bosons. These changes are [41–44], for $H(p_H) \to f(p_1)f(p_2)V(p_3)$,

$$\Gamma(H \to VV^*) = \int_0^{(M_H - M_V)^2} dm_{12}^2 \int_{m_{23,l}^2}^{m_{23,u}^2} dm_{23}^2 \frac{|\bar{\mathcal{M}}|^2}{(2\pi)^3 32 M_H^3}, \tag{14a}$$

with $m_{ij}^2 = (p_i + p_j)^2$ and, assuming massless fermions f,

$$m_{12}^2 + m_{23}^2 + m_{13}^2 = M_H^2 + M_V^2. \tag{14b}$$

The limits of the m_{23}^2 integration are

$$\lambda(m_{12}, M_H, M_V) = m_{12}^4 - 2m_{12}^2(M_H^2 + M_V^2) + (M_H^2 - M_V^2)^2, \tag{14c}$$

with

$$2m_{23,l,u}^2 = M_H^2 + M_V^2 - m_{12}^2 \mp \sqrt{\lambda(m_{12}, M_H, M_V)}. \tag{14d}$$

For the results in the next section, again, we limit ourselves to the linear order in the HEFT coefficients, i.e., the spin-summed/averaged matrix element $|\bar{\mathcal{M}}|^2$ only contains interactions $\sim a_i$ given in Table I. Turning to the $H \to \gamma\gamma$ decay width, the scattering amplitude is therefore given as

$$\mathcal{M} = |\mathcal{M}_{\text{1-loop}}|^2 + 2\text{Re}\left(\mathcal{M}_{\text{HEFT}}^* \mathcal{M}_{\text{1-loop}}\right), \tag{15}$$

where $\mathcal{M}_{\text{1-loop}}$ is the one-loop amplitude calculated with the leading-order Lagrangian given in Eq. (9) (includes parameters ζ_1 and a_{1t}) and $\mathcal{M}_{\text{HEFT}}$ is the amplitude generated with HEFT operators given in Table I. This gives rise to the $H \to \gamma\gamma$ modification and, similarly, $H \to \gamma Z, gg$ can be derived. We do not repeat this here but refer the interested readers to the existing literature [23–25], which we have cross-checked our results against. The detailed expressions of the Higgs decay widths and the contribution to the total Higgs width are listed in the Appendix.

IV. OFF-SHELLNESS AS A PROBE OF NONLINEARITY

With amplitudes and HEFT-SMEFT relations in place, we can now turn to a quantitative estimate of the sensitivity of the off-shell measurement to Higgs boson nonlinearity. To this end, we assume 85% efficiency of the 4ℓ sample after selection including a flat 29% systematic following [45,46]. To gain a qualitative statistical understanding of

expected constraints, we include these as binned χ^2 test statistic,

$$\chi^2 = \sum_i \frac{(N_i - N_i^{\rm SM})^2}{\sigma_{i,\rm syst}^2 + \sigma_{i,\rm stat}^2}, \tag{16}$$

where N_i denotes the entries in the ith bin of the off-shell Higgs momentum distribution with HEFT contributions. For ZZ processes, we have applied a cut of $q > 300$ GeV on the invariant ZZ mass. The variable $N_i^{\rm SM}$ denotes the SM expectation in bin i, and $\sigma_{i,\rm stat}$ and $\sigma_{i,\rm syst}$ are the statistical and systematic uncertainties, respectively. We approximate these with $\sigma_{i,\rm stat} = \sqrt{N_i^{\rm SM}}$ and $\sigma_{i,\rm syst} = 0.29 N_i^{\rm SM}$. The latter term includes uncertainties in background processes [49], for example from continuum production of the form $q\bar{q} \to 4\ell$.

To include the constraints from on-shell Higgs data, using the modifications in the Higgs partial decay widths, the total Higgs decay width is calculated (expressions are listed in the Appendix). With these, the modified Higgs branching ratios are given as

$$\frac{\mathrm{BR}^{\rm HEFT}(H \to X)}{\mathrm{BR}^{\rm SM}(H \to X)} = \frac{\Gamma^{\rm HEFT}(H \to X)}{\Gamma^{\rm SM}(H \to X)} \frac{\Gamma_H^{\rm SM}}{\Gamma_H^{\rm HEFT}}. \tag{17}$$

Here X denotes $\gamma\gamma$, VV^*, and γZ.[1] Combining these branching ratios with the change in the production cross section of gluon-gluon fusion and assuming narrow width approximation, the modified signal strengths are obtained as

$$\mu_{\rm ggF}^X = \frac{[\sigma_{\rm ggF}\mathrm{BR}(H \to X)]^{\rm HEFT}}{[\sigma_{\rm ggF}\mathrm{BR}(H \to X)]^{\rm SM}}. \tag{18}$$

The on-shell χ^2 statistic constructed using the signal strengths from 139 fb^{-1} data [47] is given as

$$\chi^2_{\text{on-shell}} = \sum_{i,j=1}^{\rm data} (\mu_{i,\rm exp} - \mu_{i,\rm th})(V_{ij})^{-1}(\mu_{j,\rm exp} - \mu_{j,\rm th}). \tag{19}$$

Here, $\mu_{\rm th}$ are the theory expressions incorporating the effects of HEFT operators. $\mu_{\rm exp}$ are the central values of the experimental measurements and the covariance matrix $V = \rho_{ij}\sigma_i\sigma_j$ with ρ being the correlation matrix and σ the uncertainties. To obtain an estimate of the improvements expected in future HL-LHC runs, we take the projections to 3 ab^{-1} from the recent HL-LHC analysis of Ref. [48]. The details of the signal strengths measurements are provided in the Appendix for completeness.

We can now turn to our results. To make a qualifying statement about linearity vs nonlinearity, we profile the SMEFT contributions detailed in Sec. III B.[2] This way, we obtain a statistical measure of nonlinearity as expressed through the sensitivity to the corresponding HEFT coefficients. While interactions like $a_{\Box\Box}$ enter as a uniform coupling rescaling, it is predominantly probed in the off-shell region. The on-shell region therefore probes predominantly on-shell related quantities whereas the energy-related scaling of HEFT vs SMEFT is visibly expressed by, e.g., $a_{\Box\Box}$. We have also included the $H \to WW$ off-shell region; due to its less straightforward final state phenomenology, this mode has received less attention compared to the fully reconstructible $H \to ZZ \to 4\ell$ final states. (Some of the selection criteria, see e.g., [39], also lead to a significant reduction of the off-shell region). Assuming the same (perhaps optimistic) systematic uncertainties and efficiencies as for $H \to 4\ell$, we do not find a significant information gain when including $H \to WW$ through the transverse mass observable.

We combine the on- and off-shell contributions to a total χ^2 statistic to understand the on-shell vs off-shell effects, treating these phase space regions as statistically uncorrelated. The total number of data points upon combining on-shell signal strength data with the off-shell binned data is 76 (75) for HL-LHC (LHC). To obtain the 95% C.L. regions, we constrain the χ^2 statistic with the $\Delta\chi^2$ values obtained from the degrees of freedom, i.e., (number of data points—number of parameters). After profiling over the SMEFT directions, for our all dataset (i.e., then on-shell/off-shell combination), the strongest bounds can be imposed on the operators parametrized by $a_{\Box\Box}$, a_{H13}, $a_{\Box VV}$ and a_{d4} (when these are considered in isolation). Using pairwise combinations of these operators, we show the two-dimensional parameter space allowed at 95% C.L. with both 139 fb^{-1} and 3 ab^{-1} data in Figs. 2 and 3. The constraints used for the regions are outlined in Table II for different combinations of datasets considered in the analysis (again the remaining HEFT directions are assumed to be zero).[3] The most stringent impact indeed arises from the inclusion of the off-shell measurements, shown by the red dashed contour (predominantly $H \to ZZ$) in Fig. 2.

The HL-LHC extrapolation rests on the YR18 systematic uncertainties which include a scaling of systematic uncertainties with the root of the collected luminosity. This is relatively pessimistic and it is therefore not unlikely that systematics become under much better control than what can be forecast now. In such a situation we can expect stronger limits on the BSM coupling space across many

[1]The modifications to the $b\bar{b}$ partial width are ignored in our analysis. For the total decay width, in addition to the corrections to these partial decay widths, we also scale the rest of the decay widths with the Higgs field redefinition factor. We rescale the leading-order results to reproduce the SM expectation of [11].

[2]Here 'profiling' refers to minimizing the χ^2 simultaneously using HEFT operators (a_{1t}, a_{HWW}, a_{HBB}) which are related to SMEFT operators, see Eq. (12).

[3]The allowed parameter space is extremely large after profiling over all HEFT operators.

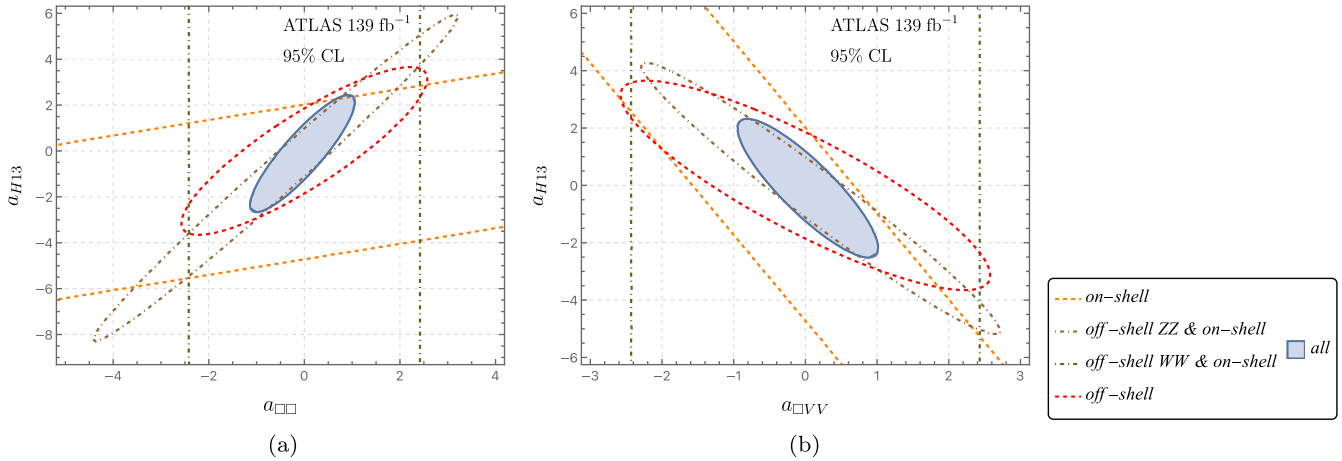

FIG. 2. 95% C.L. contours obtained for the HEFT coefficients using the ATLAS 139 fb^{-1} data. These regions are obtained after profiling over SMEFT WCs.

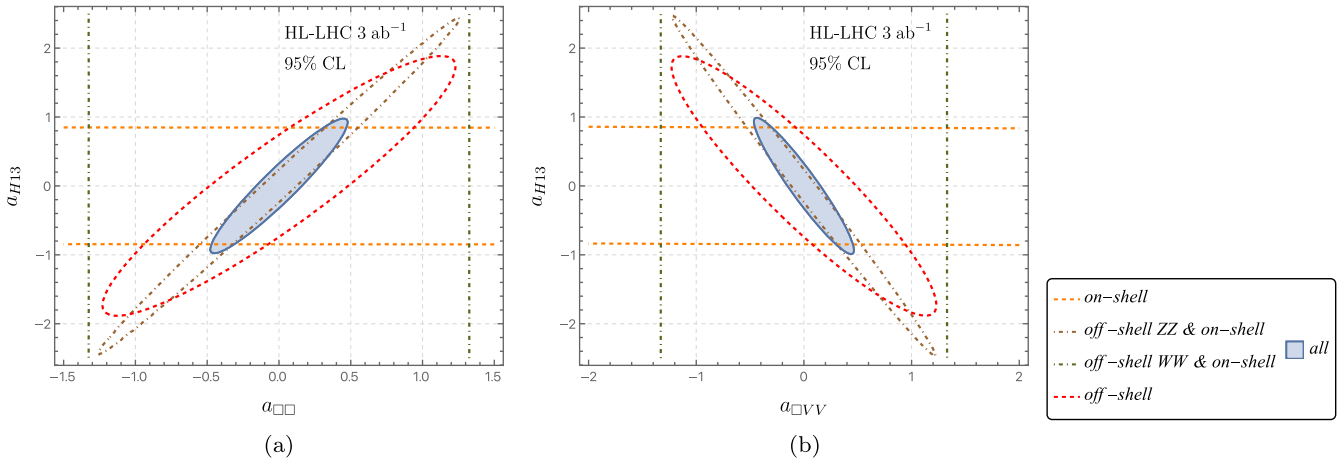

FIG. 3. Two-dimensional allowed 95% C.L. regions for the HEFT coefficients using the χ^2 analysis from the HL-LHC projected data. The HL-LHC extrapolations do not include correlations. $\chi^2_{\rm SM} = 0$ results in the tilt of the on-shell-only constraints compared to Fig. 2.

relevant Higgs production and decay modes, beyond the off-shell measurement detailed here. Of course, the relatively small data set that we have considered in this proof-of-principle analysis is not large enough to control all relevant HEFT Higgs interactions and a global fit of the discussed modes will have little sensitivity. However, the inclusion of weak boson fusion and multi-Higgs final states will add further sensitivity. Weak boson fusion appears to be particularly motivated as our discussion will directly generalise to WW scattering. We leave this, as well as a more global fit, for future work.

TABLE II. $\Delta\chi^2$ constraints used to obtain 95% C.L. regions depending on the total degrees of freedom.

	$\Delta\chi^2$ values	
Datasets	ATLAS 139 fb^{-1}	HL-LHC 3 ab^{-1}
on-shell	3.84	5.99
off-shell ZZ & on-shell	49.80	50.99
off-shell WW &on-shell	54.57	55.76
off-shell	90.53	90.53
all	93.95	95.08

V. CONCLUSIONS

The nondecoupling Higgs contribution in $gg \to VV$ production is a versatile tool to gain sensitivity to new physics beyond the Standard Model. Any deviation from expected SM coupling patterns filters through to modified tail contributions as a consequence of the interplay of absorptive amplitude parts that, in the SM, are determined by unitarity and, hence, renormalizablilty [13] from various angles. The most prevailing of these interpretations is the phrasing of off-shell constraints as on-shell measurements,

which has brought this measurement to the fame it deserves [12]. Such directions of interpretation rest on limiting assumptions [49] which suggest alternative ways of reporting outcomes of the measurement. To entice ATLAS and CMS to consider different avenues of interpretation, in this work, we have analyzed the off-shell vs on-shell correlation as a probe of Higgs boson nonlinearity. Analyses that aim to distinguish linear from nonlinear Higgs EFT modifications are typically focused on a comparison of Higgs multiplicities [1–3] (see also the recent [50,51]). In this exploratory study, we have shown that $gg \to VV$ straddles dual roles of fingerprinting unitarity departures *as well as* deviations from SMEFT attributed to the propagation of the Higgs boson. These implications generalise to weak boson fusion where we can expect similar patterns in a HEFT vs SMEFT comparison.

Of course, we can always consider additional operators, whether they appear as part of a higher-dimensional SMEFT contribution, couplings of higher chiral dimension, or as part of a plethora of operators in a global fit. In this work we have limited ourselves to top-related interactions. Contact interactions $\sim ggH$ have not been considered, but it is known that these can be separated from top-mediated processes by resolving the top loop via $H+\text{jet}$ production [52,53]. By profiling the SMEFT directions, we have obtained a statistical estimate of the constraints on non-SMEFT interactions that can be obtained, and this shows promise for the inclusion in a more comprehensive analysis, which we leave for future work.

ACKNOWLEDGMENTS

A is funded by the Leverhulme Trust under RPG-2021-031. C. E. is supported by the UK Science and Technology Facilities Council (STFC) under Grant No. ST/X000605/1 and the Leverhulme Trust under RPG-2021-031. R. K. is supported by the Helmholtz Association under the Contract No. W2/W3-123. M. S. is supported by the STFC under Grant No. ST/P001246/1.

APPENDIX: HIGGS BOSON DECAY WIDTHS AND LHC SIGNAL STRENGTH CONSTRAINTS

The contribution of HEFT operators to the Higgs decay widths relative to the SM are listed below. The contribution to the gluon-gluon fusion production cross-section relative to SM is similar to $H \to gg$,

$$\begin{aligned}
\frac{\Gamma^{\rm HEFT}(H\to ZZ)}{\Gamma^{\rm SM}(H\to ZZ)} &= 1 + 0.059a_{\Box 0} - 0.99a_{\Box\Box} + 0.99a_{\Box VV} - 0.09a_{d1} + 0.32a_{d2} + 0.64a_{d4} + 0.17a_{H13} + 0.007a_{HBB} \\
&\quad + 0.09a_{HWW} + 2\zeta_1, \\
\frac{\Gamma^{\rm HEFT}(H\to WW)}{\Gamma^{\rm SM}(H\to WW)} &= 1 - 0.99a_{\Box\Box} + 0.99a_{\Box VV} + 0.40a_{d2} + 0.05a_{HWW} + 2\zeta_1, \\
\frac{\Gamma^{\rm HEFT}(H\to \gamma\gamma)}{\Gamma^{\rm SM}(H\to \gamma\gamma)} &= 1 - 0.57a_{1t} - 0.99a_{\Box\Box} + 48.67a_{HBB} + 48.67a_{HWW} + 2.57\zeta_1, \\
\frac{\Gamma^{\rm HEFT}(H\to \gamma Z)}{\Gamma^{\rm SM}(H\to \gamma Z)} &= 1 - 0.12a_{1t} - 0.99a_{\Box\Box} + 16.26a_{d1} + 16.26a_{d2} + 32.52a_{d4} - 14.43a_{HBB} + 50.61a_{HWW} + 2.12\zeta_1, \\
\frac{\Gamma^{\rm HEFT}(H\to gg)}{\Gamma^{\rm SM}(H\to gg)} &= 1 + 2a_{1t} - 0.99a_{\Box\Box}.
\end{aligned} \tag{A1}$$

Using the above expressions, the HEFT contribution to the total Higgs decay width is

$$\begin{aligned}
\frac{\Gamma_H^{\rm HEFT}}{\Gamma_H^{\rm SM}} &= 1 + 0.17a_{1t} + 0.001a_{\Box 0} - 0.99a_{\Box\Box} + 0.24a_{\Box VV} \\
&\quad + 0.02a_{d1} + 0.12a_{d2} + 0.07a_{d4} + 0.004a_{H13} \\
&\quad + 0.09a_{HBB} + 0.20a_{HWW} + 0.5\zeta_1.
\end{aligned} \tag{A2}$$

The signal strength measurements used in the $\chi^2_{\rm onshell}$ for 139 fb^{-1} data along with correlation matrix are shown in Table III. The HL-LHC 3 ab^{-1} projections of the signal strengths are shown in column 4.

TABLE III. Details of the signal strength measurements used in the $\chi^2_{\text{on-shell}}$. Columns 2 and 3 list the ATLAS 139 fb^{-1} data. Column 4 lists the projections used for HL-LHC 3 ab^{-1}.

	ATLAS Run 2 data [47]				
Observables	Measurements	Correlations			HL-LHC uncertainties [48]
$\mu_{ggF}^{\gamma\gamma}$	$1.02^{+0.11}_{-0.11}$	1	0.05	0.09	± 0.36
μ_{ggF}^{ZZ}	$0.95^{+0.11}_{-0.11}$		1	0.1	± 0.039
μ_{ggF}^{WW}	$1.13^{+0.13}_{-0.12}$			1	± 0.043
$\mu_{ggF}^{Z\gamma}$					± 0.33

[1] R. Gómez-Ambrosio, F. J. Llanes-Estrada, A. Salas-Bernárdez, and J. J. Sanz-Cillero, SMEFT is falsifiable through multi-Higgs measurements (even in the absence of new light particles), Commun. Theor. Phys. **75**, 095202 (2023).

[2] A. Bhardwaj, C. Englert, D. Gonçalves, and A. Navarro, Nonlinear *CP* violation in the top-Higgs sector, Phys. Rev. D **108**, 115006 (2023).

[3] R. L. Delgado, R. Gómez-Ambrosio, J. Martínez-Martín, A. Salas-Bernárdez, and J. J. Sanz-Cillero, Production of two, three, and four Higgs bosons: Where SMEFT and HEFT depart, arXiv:J. High Energy Phys. 03 (2024) 037.

[4] T. Appelquist and C. W. Bernard, Strongly Interacting Higgs Bosons, Phys. Rev. D **22**, 200 (1980).

[5] A. C. Longhitano, Heavy Higgs bosons in the Weinberg-Salam model, Phys. Rev. D **22**, 1166 (1980).

[6] A. C. Longhitano, Low-energy impact of a heavy Higgs boson sector, Nucl. Phys. **B188**, 118 (1981).

[7] F. Feruglio, The chiral approach to the electroweak interactions, Int. J. Mod. Phys. A **08**, 4937 (1993).

[8] I. Brivio, T. Corbett, O. J. P. Éboli, M. B. Gavela, J. Gonzalez-Fraile, M. C. Gonzalez-Garcia, M. C. Gonzalez-Garcia, L. Merlo, and S. Rigolin, Disentangling a dynamical Higgs, J. High Energy Phys. 03 (2014) 024.

[9] G. Buchalla, O. Catà, and C. Krause, Complete electroweak chiral Lagrangian with a light Higgs at NLO, Nucl. Phys. **B880**, 552 (2014); **B913**, 475(E) (2016).

[10] G. Buchalla, O. Catá, and C. Krause, On the power counting in effective field theories, Phys. Lett. B **731**, 80 (2014).

[11] S. Dittmaier *et al.* (LHC Higgs Cross Section Working Group), Handbook of LHC Higgs Cross Sections: 1. Inclusive Observables, arXiv:arXiv:1101.0593.

[12] F. Caola and K. Melnikov, Constraining the Higgs boson width with ZZ production at the LHC, Phys. Rev. D **88**, 054024 (2013).

[13] N. Kauer and G. Passarino, Inadequacy of zero-width approximation for a light Higgs boson signal, J. High Energy Phys. 08 (2012) 116.

[14] G. F. Giudice, C. Grojean, A. Pomarol, and R. Rattazzi, The strongly-interacting light Higgs, J. High Energy Phys. 06 (2007) 045.

[15] J. D. Wells and Z. Zhang, Effective theories of universal theories, J. High Energy Phys. 01 (2016) 123.

[16] C. Englert, G. F. Giudice, A. Greljo, and M. Mccullough, The $\hat{H}$-parameter: An oblique Higgs view, J. High Energy Phys. 09 (2019) 041.

[17] B. Henning, X. Lu, and H. Murayama, How to use the standard model effective field theory, J. High Energy Phys. 01 (2016) 023.

[18] C. Englert, R. Kogler, H. Schulz, and M. Spannowsky, Higgs characterisation in the presence of theoretical uncertainties and invisible decays, Eur. Phys. J. C **77**, 789 (2017).

[19] G. Buchalla, O. Cata, and C. Krause, A systematic approach to the SILH Lagrangian, Nucl. Phys. **B894**, 602 (2015).

[20] Anisha, S. Das Bakshi, C. Englert, and P. Stylianou, Higgs boson footprints of hefty ALPs, Phys. Rev. D **108**, 095032 (2023).

[21] I. Brivio, O. J. P. Éboli, M. B. Gavela, M. C. Gonzalez-Garcia, L. Merlo, and S. Rigolin, Higgs ultraviolet softening, J. High Energy Phys. 12 (2014) 004.

[22] M. J. Herrero and R. A. Morales, One-loop renormalization of vector boson scattering with the electroweak chiral Lagrangian in covariant gauges, Phys. Rev. D **104**, 075013 (2021).

[23] M. Herrero and R. A. Morales, Anatomy of Higgs boson decays into $\gamma\gamma$ and γZ within the electroweak chiral Lagrangian in the R_ξ gauges, Phys. Rev. D **102**, 075040 (2020).

[24] Anisha, O. Atkinson, A. Bhardwaj, C. Englert, and P. Stylianou, Quartic gauge-Higgs couplings: Constraints and future directions, J. High Energy Phys. 10 (2022) 172.

[25] M. J. Herrero and R. A. Morales, One-loop corrections for WW to HH in Higgs EFT with the electroweak chiral Lagrangian, Phys. Rev. D **106**, 073008 (2022).

[26] J. M. Dávila, D. Domenech, M. J. Herrero, and R. A. Morales, Exploring correlations between HEFT Higgs couplings κ_V and κ_{2V} via HH production at e^+e^- colliders, arXiv:2312.03877.

[27] C. Englert, W. Naskar, and D. Sutherland, BSM patterns in scalar-sector coupling modifiers, J. High Energy Phys. 11 (2023) 158.

[28] G. Buchalla, O. Cata, A. Celis, and C. Krause, Standard model extended by a heavy singlet: Linear vs nonlinear EFT, Nucl. Phys. **B917**, 209 (2017).

[29] F. Arco, D. Domenech, M. J. Herrero, and R. A. Morales, Nondecoupling effects from heavy Higgs bosons by matching 2HDM to HEFT amplitudes, Phys. Rev. D **108**, 095013 (2023).

[30] S. Dawson, D. Fontes, C. Quezada-Calonge, and J. J. Sanz-Cillero, Is the HEFT matching unique?, arXiv:Phys. Rev. D **109**, 055037 (2024).

[31] M. E. Peskin and T. Takeuchi, Estimation of oblique electroweak corrections, Phys. Rev. D **46**, 381 (1992).

[32] I. Brivio, J. Gonzalez-Fraile, M. C. Gonzalez-Garcia, and L. Merlo, The complete HEFT Lagrangian after the LHC Run I, Eur. Phys. J. C **76**, 416 (2016).

[33] L. Berthier and M. Trott, Towards consistent electroweak precision data constraints in the SMEFT, J. High Energy Phys. 05 (2015) 024.

[34] L. Bellafronte, S. Dawson, and P. P. Giardino, The importance of flavor in SMEFT electroweak precision fits, J. High Energy Phys. 05 (2023) 208.

[35] B. Grzadkowski, M. Iskrzynski, M. Misiak, and J. Rosiek, Dimension-six terms in the standard model Lagrangian, J. High Energy Phys. 10 (2010) 085.

[36] K. Hagiwara, R. D. Peccei, D. Zeppenfeld, and K. Hikasa, Probing the weak boson sector in $e^+e^- \to W^+W^-$, Nucl. Phys. **B282**, 253 (1987).

[37] K. Arnold *et al.*, VBFNLO: A Parton level Monte Carlo for processes with electroweak bosons, Comput. Phys. Commun. **180**, 1661 (2009).

[38] J. Baglio *et al.*, Release Note—VBFNLO2.7.0, arXiv:1404.3940.

[39] J. M. Campbell, R. K. Ellis, and C. Williams, Bounding the Higgs width at the LHC: Complementary results from $H \to WW$, Phys. Rev. D **89**, 053011 (2014).

[40] J. M. Campbell, R. K. Ellis, and C. Williams, Bounding the Higgs width at the LHC using full analytic results for $gg- > e^-e^+\mu^-\mu^+$, J. High Energy Phys. 04 (2014) 060.

[41] T. G. Rizzo, Decays of heavy Higgs bosons, Phys. Rev. D **22**, 722 (1980).

[42] W.-Y. Keung and W. J. Marciano, Higgs scalar decays: $H \to W^{\pm}X$, Phys. Rev. D **30**, 248 (1984).
[43] S. Dawson, C. Englert, and T. Plehn, Higgs physics: It ain't over till it's over, Phys. Rep. **816**, 1 (2019).
[44] S. Dawson and P. P. Giardino, Higgs decays to ZZ and $Z\gamma$ in the standard model effective field theory: An NLO analysis, Phys. Rev. D **97**, 093003 (2018).
[45] C. Englert, R. Kogler, H. Schulz, and M. Spannowsky, Higgs coupling measurements at the LHC, Eur. Phys. J. C **76**, 393 (2016).
[46] A. Hayrapetyan *et al.* (CMS Collaboration), Measurement of the Higgs boson mass and width using the four leptons final state, Technical Report, 2023.
[47] G. Aad *et al.* (ATLAS Collaboration), Combined measurements of Higgs boson production and decay using up to 139 fb^{-1} of proton-proton collision data at $\sqrt{s} = 13$ TeV collected with the ATLAS experiment, Technical Report ATLAS-CONF-2021-053, 2021, http://cds.cern.ch/record/2789544.
[48] A. Dainese, M. Mangano, A. B. Meyer, A. Nisati, G. Salam, and M. A. Vesterinen, Report on the physics at the HL-LHC, and perspectives for the HE-LHC, Technical Report, 2019, 10.23731/CYRM-2019-007.
[49] C. Englert, Y. Soreq, and M. Spannowsky, Off-shell Higgs coupling measurements in BSM scenarios, J. High Energy Phys. 05 (2015) 145.
[50] P. Stylianou and G. Weiglein, Constraints on the trilinear and quartic Higgs couplings from triple Higgs production at the LHC and beyond, arXiv:Eur. Phys. J. C **84**, 366 (2024).
[51] A. Papaefstathiou and G. Tetlalmatzi-Xolocotzi, Multi-Higgs boson production with anomalous interactions at current and future proton colliders, arXiv:2312.13562.
[52] A. Banfi, A. Martin, and V. Sanz, Probing top-partners in Higgs + jets, J. High Energy Phys. 08 (2014) 053.
[53] C. Grojean, E. Salvioni, M. Schlaffer, and A. Weiler, Very boosted Higgs in gluon fusion, J. High Energy Phys. 05 (2014) 022.